

# Chapter 1

## Introduction

### 1.1 An overview of the liquid crystalline phase

The type of ordering of the constituent molecules of condensed phases characterizes the phase. In condensed phases made up of anisotropic molecules one can define both positional and orientational ordering of the constituent molecules. In certain condensed matter systems, comprised of molecules with a high degree of shape anisotropy, the crystalline phase melts into an intermediate phase which, on further heating undergoes a transition to an isotropic phase. This intermediate phase which possesses properties characteristic of both crystals and liquids like elasticity, viscosity, surface tension etc., is called the *liquid crystalline* phase. In this thesis we shall be mainly concerned with properties of materials in the liquid crystalline phases. Even within the liquid crystalline phases one can have various types of ordering leading to distinct liquid crystalline sub-phases. In general two types of anisotropically shaped molecules show liquid crystalline phases, 'rod-like' molecules and 'disc-shaped' molecules.

Liquid crystals have gained a lot of importance in recent times due to their practical applications. One of the widest areas of application of liquid crystals is in display technology. The performance of liquid crystal displays (LCDs) depends on the viscoelastic properties of the material used in the display. This thesis describes the study of viscoelastic coefficients using the dynamic light scattering technique. Apart from LCDs, there are other applications of liquid crystals, for example, in appropriate geometries, liquid crystals can also be used as tunable phase retarders, rotators

and diffraction gratings. Such tunable optical components are very useful in optical signal transmission systems. We discuss the properties of one such device, a liquid crystal phase grating, in chapter 5 of this thesis.

Liquid crystals in which phase transitions can be brought about by changing the temperature are called *thermotropic* liquid crystals. A vast majority of liquid crystalline compounds fall in this category. There is another class of liquid crystals made up of multicomponent systems which also show a rich variety of phases. These systems are called *lyotropic* liquid crystals and phase transitions in them can be brought about by changing either the temperature or the relative concentrations of the various components. Typically, lyotropic liquid crystals are formed by surfactant molecules dissolved in a solvent which is usually water. When surfactant molecules are brought in contact with water they organize themselves into anisotropic structures which give rise to liquid crystalline phases. In the following sections we briefly introduce some of the main features of the commonly occurring liquid crystals, like nematic, cholesteric and smectic phases.

### **1.1.1 The nematic phase**

The nematic phase is one of the most commonly occurring liquid crystalline phases. In the nematic phase, the molecules have long range orientational order but no positional ordering. A schematic representation of the molecular ordering in the isotropic phase is shown in figure(1.1 a)

In cases where the molecules are of rod-like shape, the long axis of the molecules point, on an average, along a particular direction in space. We usually use a unit vector  $n$  along the average direction of molecular orientation. This vector is also called the director. This is shown in figure(1.1 b). The rod-like molecules are free to rotate about their long axis and to a much lesser extent about their short axes. The typical rotational frequencies about their short axes in the range  $10^5$  to  $10^6$  Hz and about the long axis in the range  $10^{11}$  to  $10^{12}$  Hz. The probability of finding a molecule parallel and anti-parallel to the director is the same. This gives rise to the physical

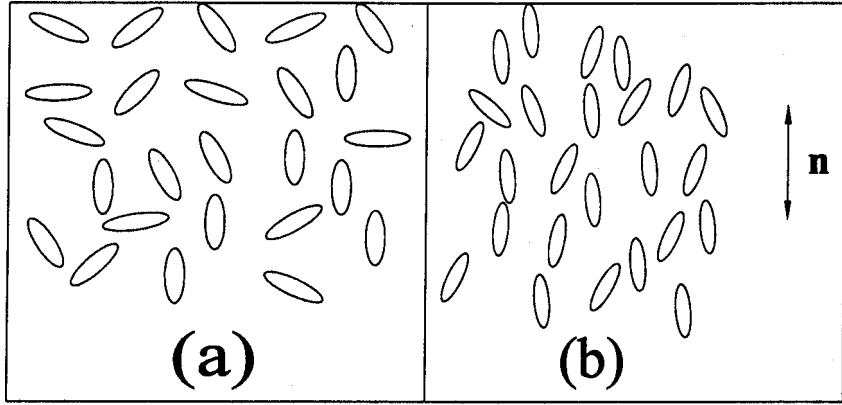


Figure 1.1: (a) Schematic representation of an isotropic fluid. Here the molecules have a random orientational and positional arrangement. (b) Schematic representation of the molecular arrangement in the nematic phase. Here, the average direction of orientation is along an apolar unit vector denoted by  $\mathbf{n}$ , called the director.

equivalence of  $\mathbf{n}$  and  $-\mathbf{n}$ . Further the nematic phase has cylindrical symmetry about the director. The degree of orientational ordering of the molecules in the nematic phase can be defined by an order parameter  $S$ . The order parameter is a function of temperature. In literature this order parameter is defined by:

$$S = \frac{1}{2} \langle 3\cos^2(\theta_i) - 1 \rangle$$

Where  $\theta_i$  is the angle made by the  $i^{\text{th}}$  molecule with the director and the angular brackets indicate a spatial average. Typical values of the nematic order parameters are between 0.4 and 0.7.

### 1.1.2 The cholesteric phase

In the case of nematics where the constituent molecules are chiral, or in the case of nematics doped with chiral molecules, the structure acquires a spontaneous twist. This results in a helical structure of a definite pitch. In such structures the director gradually rotates about an axis perpendicular to itself. The cholesteric structure is depicted in figure(1.2).

If we consider the  $z$  axis to lie parallel to the helix axis and the director to be in the  $x$ - $y$  plane, the cholesteric can be described by the following director components

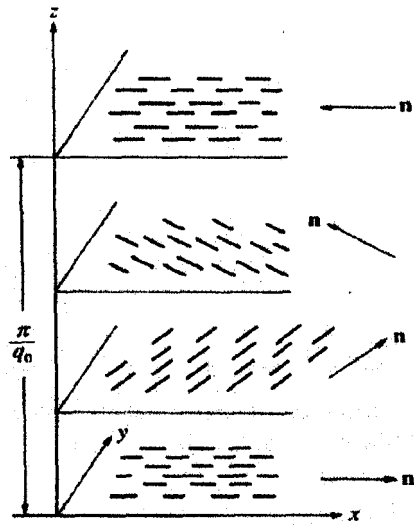


Figure 1.2: A Schematic figure of the molecular arrangement in the cholesteric phase, The director rotates about an axis perpendicular to itself giving rise to a helical structure with pitch  $P$ .  $P = 2\pi/q_0$  here,  $q_0$  is the wavevector of the cholesteric.

$$n_x = \cos(q_0 z)$$

$$n_y = \sin(q_0 z)$$

$$n_z = 0$$

Where  $q_0 = 2\pi/P$  is the magnitude of the wavevector of the cholesteric of pitch  $P$ . The sign of  $q_0$  determines the handedness of the cholesteric structure. In practice, materials exhibit either left or right handed structures. The cholesteric pitch depends on the degree of chirality of the molecules and the temperature of the system. When the pitch becomes comparable to the wavelength of light, Bragg reflection occurs, resulting in the characteristic iridescent appearance of cholesterics when viewed in white light.

### 1.1.3 The smectic phases

In smectic phases, molecules arrange themselves in layers giving rise to a one dimensional quasi-long positional ordering. Landau and Peierls showed that true one dimensional long range translational ordering at *any* finite temperature is not possible due to the presence of thermal fluctuations. The result is a layered structure

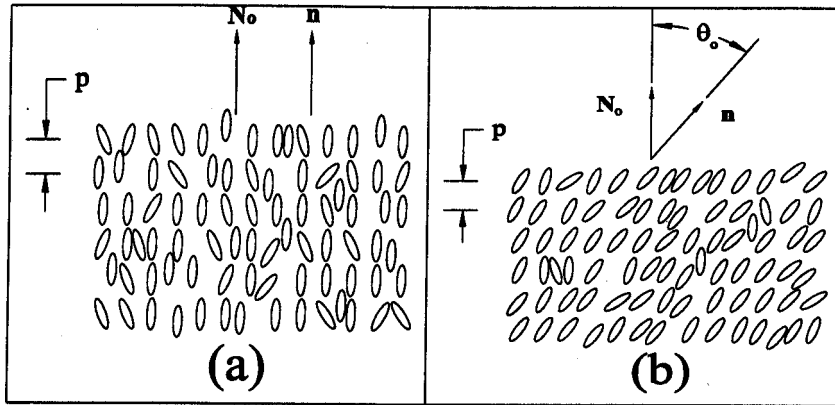


Figure 1.3: The smectic phases have layered structures. (a) When the director is parallel to the layer normal the phase is called Smectic A. (b) If the director is uniformly tilted with respect to the layer normal the phase is called Smectic C.

with quasi long range translational order in a direction parallel to the layer normal and liquid like positional order within the layers.

### Smectic A

In the smectic A phase the molecules arrange themselves in layers with the director normal to the layers. The phase is macroscopically uniaxial with the axis of cylindrical symmetry along the layer normal  $N$ . This is depicted in figure(1.3a).

### Smectic C

The structure of the smectic C phase is very similar to the smectic A phase except for the fact that the molecules in all the layers are tilted in the same direction with respect to the layer normal  $N$ , as shown in figure(1.3b). Due to this tilt the director develops a component in the plane of the layers. The projection of the director  $n$  on the layer is called the  $c$  vector.

### Smectic C\*

In smectic C, if the molecules are chiral, or if there are chiral dopants, the structure develops a spontaneous twist about its layer normal leading to the Smectic C\* phase or the chiral smectic C phase where  $n$  precesses continuously about the layer normal.

Since the macroscopic structure lacks a mirror plane, the phase can be locally ferroelectric by sustaining in each layer a permanent electric dipole moment perpendicular to the twist axis and the  $c$  vector.

Liquid crystalline phases can also be formed out of disk like molecules. These are called the *discotic phases*.

Apart from the phases mentioned above, there are also some defect proliferated phases like the *twist grain boundary* (TGB) and the *blue* phases. The blue phases occur over a short range of temperatures close to the cholesteric-isotropic transition. The TGB phases occur between the cholesteric and smectic phases. TGB phase consists of a helical arrangement of smectic blocks separated by a twisted region, made up of linear arrays of screw dislocations. Depending upon the molecular arrangement within the smectic blocks, the TGB phases are further subdivided into TGBA, TGBC, TGBC\* etc.

## 1.2 Mechanical and optical properties

The high degree of anisotropy of liquid crystals at the molecular level is clearly reflected in the bulk optical, mechanical, dielectric and magnetic properties. Perhaps the most striking difference in mechanical properties between ordinary fluids and liquid crystals is in the nature of their viscosities. An isotropic fluid lacking preferred direction yields the same value for viscosity no matter how it is measured. However, in liquid crystals, the viscosity depends on the coupling of the director to the flow field. In fact, a nematic liquid crystal can have five independent viscosity coefficients. Liquid crystals respond to applied mechanical torques, and stresses. The elastic deformation of a nematic liquid crystal arises from torques and in general can be resolved into three basic deformations called the splay, twist and bend. These deformations are illustrated in figure(1.4). The associated elastic constants are called the Frank curvature elastic constants.

The anisotropy in optical properties is exploited in a wide range of liquid crystal applications. Macroscopic linear birefringence is a consequence of the dielectric anisotropy

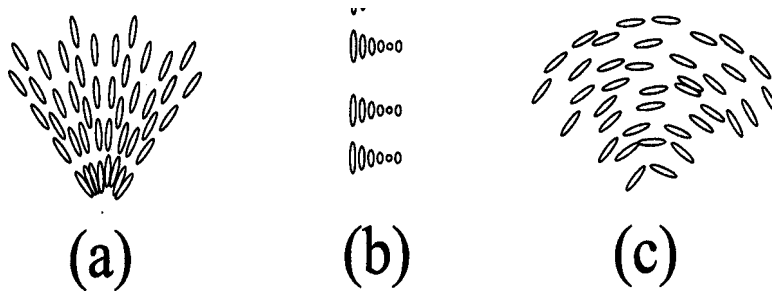


Figure 1.4: Illustrating the molecular orientation in a nematic sample subjected to the three basic deformations (a) splay, (b) twist and (c) bend. Any arbitrary deformation of the nematic can be resolved to be a combination of these three basic deformations. Splay, twist and bend are each characterized by an independent elastic constant denoted by  $K_1$ ,  $K_2$  and  $K_3$ . These constants are of the order of  $10^{-6}$  dynes.

at the molecular level. In addition to local linear birefringence some liquid crystal structures like cholesterics also possess helicity. This combination of birefringence and spatial helicity endows these liquid crystals with properties like selective Bragg reflection and diffraction.

Another important feature of liquid crystals is the intense scattering of light caused by thermal fluctuations of the director. The low value of curvature elastic constants of the liquid crystals leads to large thermal fluctuations even at ambient temperatures to create long wavelength distortions. These distortions result in refractive index variations on the length scales of the wavelength of light. Analysis shows that this process leads to strong scattering of light with a scattering cross-section  $10^6$  times that found in normal liquids. In chapters 3,4 and 6 of this thesis we are concerned with light scattering studies from nematic and cholesteric liquid crystals. We employ dynamic light scattering to investigate the modes of fluctuations of the director which in turn lead to a determination of viscoelastic coefficients.

In chapter 5 we discuss diffraction from cholesterics in the phase grating mode, in particular, the intensity profiles of the diffracted orders from non-uniform cholesteric gratings.

## 1.3 Dynamic light scattering

The scattering of light from any medium is due to the refractive index fluctuations in that medium. By analyzing the scattered light it is possible to deduce information about these fluctuations and the related material properties of the system. When a medium with such temporal refractive index fluctuations is illuminated with coherent light, a fluctuating speckle pattern is formed in the far field. The basic set up used by us for light scattering studies is shown in figure(1.5). Light from a laser, linearly polarized in a direction  $\hat{i}$  is scattered by a medium. The scattered light passes through an analyzer which selects a particular polarization  $f$  before it enters a detector. The position of the detector defines the scattering angle  $\theta$  relative to the main beam. The intersection of the incident beam and the beam detected by the detector defines the scattering volume  $V$  involved in the scattering process. The speckle pattern arises because of the interference between light waves scattered from various portions of the scattering volume. The fluctuations in the speckle pattern are due to refractive index fluctuations in the scattering volume. The detector senses the fluctuating intensity of the speckle pattern. An analysis of the intensity fluctuations reveals the director dynamics in the scattering volume.

The fluctuations are studied by analyzing the autocorrelation function of the scattered light intensity. In the next section we briefly describe the autocorrelation function of a fluctuating signal in the context of our light scattering experiments.

### 1.3.1 Fluctuations and their autocorrelation functions

Random thermal fluctuations of thermodynamic variables are commonplace in condensed matter. As an example, we consider a system comprising of many particles. Let  $A(t)$  be some property of the system at a time  $t$  that depends on the position and momenta of all the particles in the system. Due to random thermal motions the positions and momenta of the particles change constantly and this is reflected as a random fluctuation of  $A(t)$  about an average value ( $\bar{A}$ ). When observed in the time domain  $A(t)$  looks like a random noise signal. The average value of  $A$  that would be

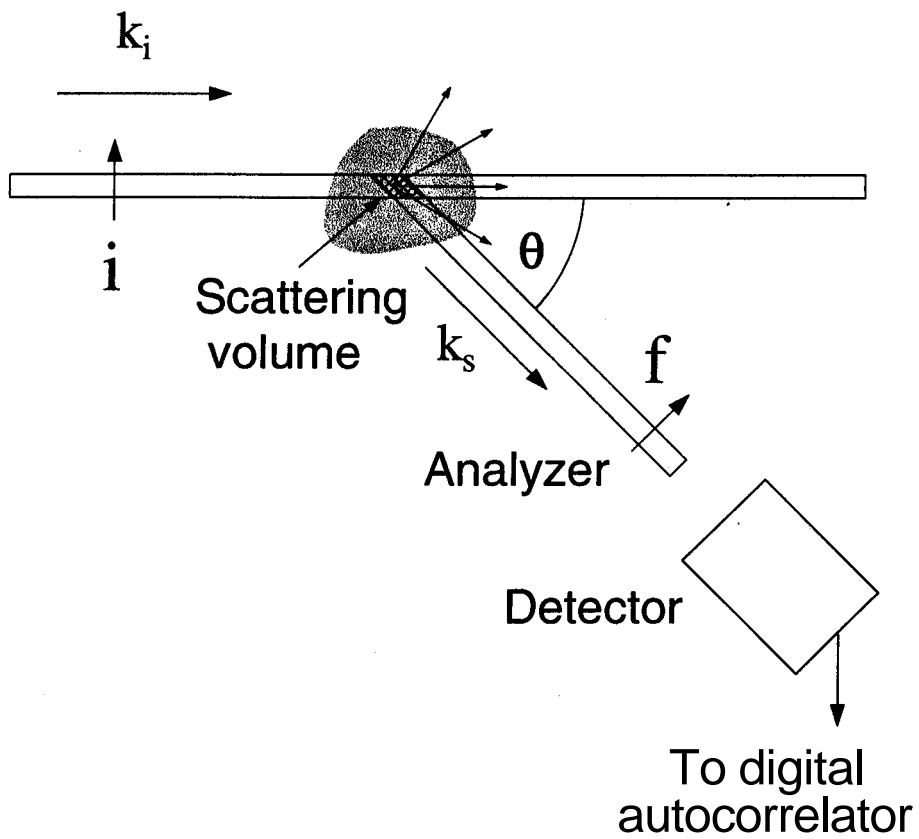


Figure 1.5: A schematic diagram of the basic arrangement of a light scattering experiment.  $\mathbf{k}_i$  is the incident wavevector in the direction  $i$  and  $\mathbf{k}_s$  is the scattered wavevector in the direction  $s$ . The plane containing  $\mathbf{k}_i$  and  $\mathbf{k}_s$  is called the scattering plane.

measured as the bulk property of the system in equilibrium is given by,

$$\langle A \rangle = \lim_{T \rightarrow \infty} \frac{1}{T} \int_0^T A(t) dt$$

Where  $T$  is the total time over which  $A(t)$  is measured. For convenience we take the average value  $\langle A \rangle$  to be zero. A *temporal correlation function* measures the degree to which two dynamical properties are correlated over a period of time. The *autocorrelation function* (ACF)  $\langle A(0)A(\tau) \rangle$  is a measure of the correlation between two values of the quantity  $A$ ,  $A(t)$  and  $A(t + \tau)$  at times  $t$  and  $t + \tau$ . Here,  $\tau$  is called the *delay time*. Mathematically the autocorrelation function of  $A(t)$  can be written as

$$\langle A(0)A(\tau) \rangle = \lim_{T \rightarrow \infty} \frac{1}{T} \int_0^T A(t)A(t + \tau) dt$$

In practice, a digital correlator is used to analyze the fluctuating intensity. It performs a discrete time autocorrelation. We define the following symbols for the discrete time autocorrelation function in analogy with the continuous time version discussed above. The time axis is divided into discrete equally spaced intervals  $\Delta t$  such that  $t = j\Delta t$ . Samples of  $A(t)$  are obtained at these intervals.

Time is now expressed as  $t = j \Delta t$  Where  $j$  is a running index that takes values 1,2,3... Delay time is expressed as  $\tau = n \Delta t$ . The two samples of  $A(t)$  are delayed by  $n$  samples. The quantity analogous to the total measurement time  $T$  is  $N \Delta t$ . Where  $N$  is the total number of samples. The delayed sample  $A(t + \tau)$  is taken at  $(j + n) \Delta t$ . The time variation of  $A$  in time is shown in figure(1.6). The sampling interval  $\Delta t$  is chosen to be small enough such that  $A(t)$  can be faithfully reproduced. The discrete time version of the average value is given by,

$$\langle A \rangle \simeq \frac{1}{N} \lim_{N \rightarrow \infty} \sum_{j=1}^N A_j$$

The autocorrelation function is given by,

$$\langle A(0)A(\tau) \rangle \simeq \frac{1}{N} \lim_{N \rightarrow \infty} \sum_{j=1}^{N-n} A_j A_{j+n} \quad (1.1)$$

For the zero delay i.e.,  $n=0$  all the terms in equation(1.1) have positive values. For

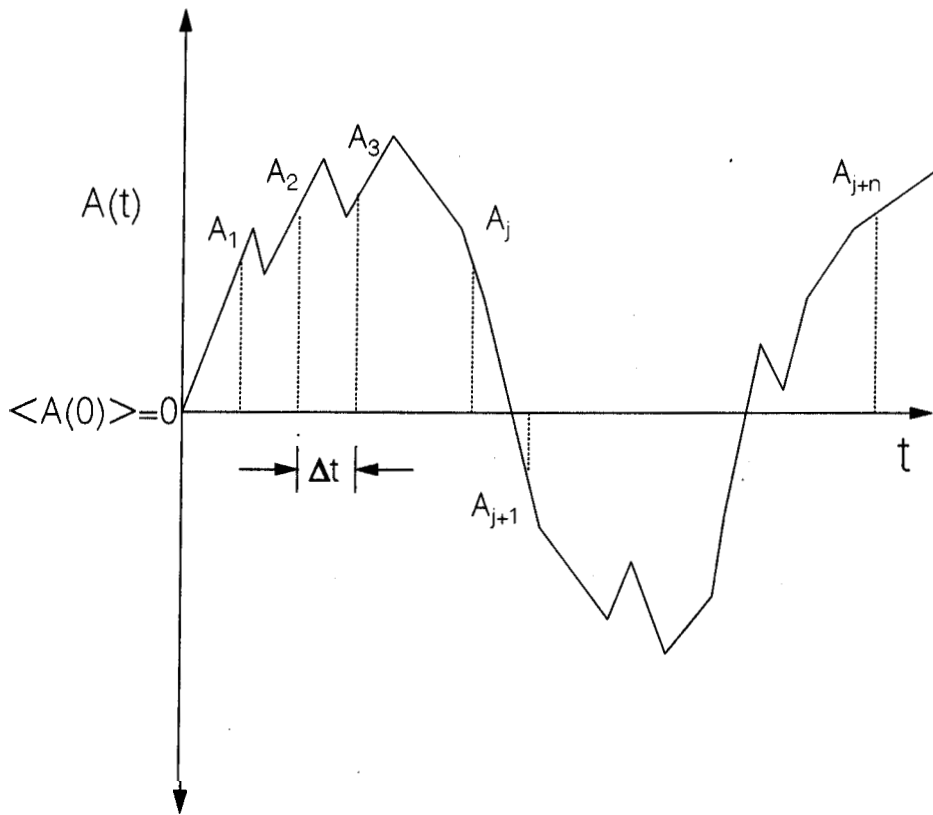


Figure 1.6: A continuous signal sampled at an interval of  $\Delta t$ .

$n \neq 0$ , the summation will have both positive and negative contributions. As  $n \rightarrow N$  for truly random signals we can expect the total positive contribution to be almost equal to the total negative contribution. This causes the autocorrelation function to decay to zero at longer times. For a random signal the ACF starts with a value

$$\langle A(0)A(\tau) \rangle = \langle A^2 \rangle \quad (1.2)$$

at  $\tau=0$ . As  $\tau \rightarrow \infty$ ,  $A(0)$  and  $A(\tau)$  become more and more uncorrelated hence

$$\langle A(0)A(\tau) \rangle \simeq \langle A(0) \rangle \langle A(\tau) \rangle = \langle A \rangle^2 \quad (1.3)$$

$A(t)$  being a stationary property. In figure(1.7a) we show a random signal and in figure(1.7b) its autocorrelation function. By examining the nature of the decay of the ACF from  $\langle A^2 \rangle$  to  $\langle A \rangle^2$  one can obtain the relaxation time of the randomly fluctuating quantity  $A(t)$ . For example if  $A(t)$  represents the intensity of the light scattered by a collection of mono-disperse spherical scatterers suspended in a solution, a single exponential function will describe the decay of the ACF of  $A(t)$ .

Typically the autocorrelation function decays as

$$\langle A(0)A(\tau) \rangle = \langle A \rangle^2 + \{ \langle A^2 \rangle - \langle A \rangle^2 \} e^{-(\tau/\tau_A)}$$

Here  $\tau_A$  is the characteristic relaxation time of the fluctuating quantity  $A(t)$ . The relaxation time is the key quantity we will be concerned with in most of the forthcoming discussions on dynamic light scattering.

In DLS experiments the aim is to extract the relaxation time by analyzing the decay of the intensity autocorrelation function. In practice, the detector of light intensity, used in the DLS experiments is a square law detector. It measures the intensity autocorrelation function of the scattered light. In the next section, we discuss the Gaussian light scattering theory which relates the **experimentally** measured intensity autocorrelation function to the electric field autocorrelation function.

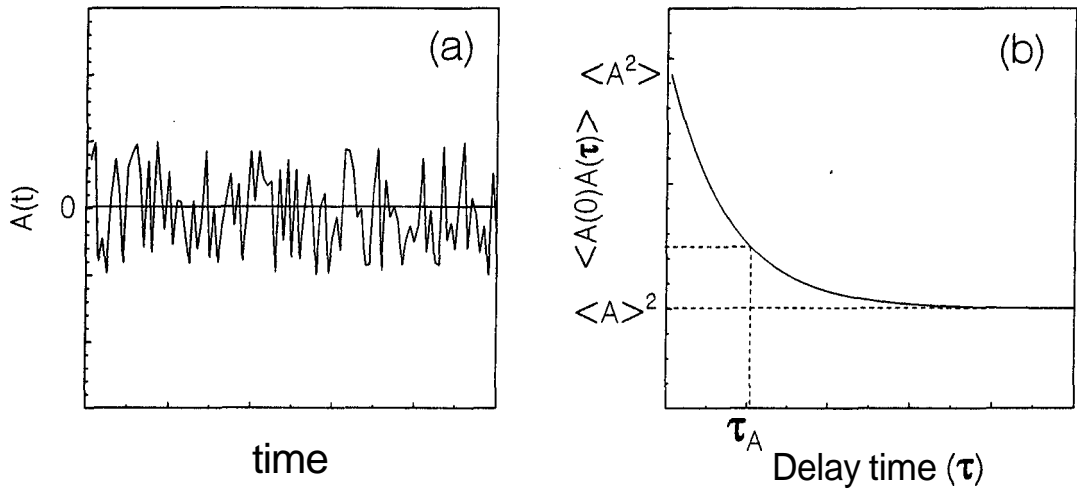


Figure 1.7: A random signal and its autocorrelation function.

### 1.3.2 Gaussian light scattering theory

We consider a beam of a finite width illuminating the sample under study. We shall consider the case of homodyne light scattering or single beam light scattering where only the light scattered from the sample reaches the detector. The scattered electric field  $E_s(t)$  is proportional to the instantaneous change in dielectric constant in the scattering volume. In a liquid crystal, the fluctuations arise due to the incessant thermal motions of the director. The scattering volume  $V$  is sub divided into sub-regions of volume small compared to the wavelength of light. The scattered field  $E_s$  arriving at the detector can be regarded as a super position of fields from each of

these sub-regions

$$E_s = \sum_n E_s^{(n)}$$

Where  $E_s^{(n)}$  is the scattered field arriving at the detector from the  $n^{\text{th}}$  sub-region. An important assumption made here is that the director or particle motions in a given sub-region are independent of those in the other sub-regions. This assumption implies that the fields emanating from each sub-region are independent of each other.  $E_s$  can be regarded as a sum of independent random variables  $E_s^{(1)}, E_s^{(2)}, E_s^{(3)} \dots$  which represent the fields emanating from the various subregions 1,2,3.... We can now invoke the central limit theorem [1] which states that the sum of a large number of independent random variables with unknown individual distribution functions must have a Gaussian distribution with zero mean. It might not always be possible to apply the central limit theorem. The scattered fields will be non-Gaussian in the presence of laser source correlations and number density fluctuations where scattering volumes are very small [2]

We shall now derive the expression for the intensity autocorrelation function that is measured in the experiment. The intensity autocorrelation function is defined as

$$\langle I_s(0)I_s(\tau) \rangle = \langle E_s(0)E_s^*(0)E_s(\tau)E_s^*(\tau) \rangle \quad (1.4)$$

We drop the subscript "s" with the understanding that E stands for the scattered electric field henceforth.

The intensity autocorrelation function is a 4<sup>th</sup> moment of the Gaussian random variable and can be written as a sum of the products of all possible 2<sup>nd</sup> moments [3].

$$\begin{aligned} \langle I(0)I(\tau) \rangle &= \langle E(0)E^*(0) \rangle \langle E(\tau)E^*(0) \rangle \\ &\quad + \langle E(0)E(\tau) \rangle \langle E^*(0)E^*(\tau) \rangle \\ &\quad + \langle E(0)E^*(\tau) \rangle \langle E^*(0)E(\tau) \rangle \\ &= \langle I \rangle^2 + |\langle E(0)E(\tau) \rangle|^2 + |\langle E(0)E^*(\tau) \rangle|^2 \end{aligned} \quad (1.5)$$

Here  $E(t)$  has the usual time dependent part  $e^{-i\omega t}$  times a slowly varying contribution due to the inelastic scattering. The product  $E(0)E(\tau)$  oscillates at the optical frequency  $2\omega$  and its time average over the time scales of interest is practically zero. Dropping the second term, the intensity autocorrelation function can be written as

$$\langle I(0)I(\tau) \rangle = \langle I \rangle^2 + |\langle E(0)E^*(\tau) \rangle|^2 \quad (1.6)$$

This is the well known Siegert relation that relates the electric field autocorrelation function to the intensity autocorrelation function. We now define the following correlation functions,

$$g_1(\tau) = \frac{\langle E(0)E^*(\tau) \rangle}{\langle I \rangle} \quad (1.7)$$

$$g_2(\tau) = \frac{\langle I(0)I(\tau) \rangle}{\langle I \rangle^2} \quad (1.8)$$

The normalized form of  $g_2(\tau)$  is defined as,

$$G_2(\tau) = \frac{g_2(\tau)}{g_2(\infty)} - 1 \quad (1.9)$$

Here,  $g_2(\infty)$  is the value of electric field autocorrelation function at very large delay times i.e., as  $\tau \rightarrow \infty$  and is known as the base line.

The basic quantity of interest here is the intensity autocorrelation function  $g_2(\tau)$ . Usually  $g_2(\tau)$  decays exponentially with the delay time  $\tau$ , with a relaxation time say,  $\tau_r$ .

Equations(1.7), (1.8) and (1.9) are the theoretical expressions for the autocorrelation functions involved in DLS experiments. In real situations, experimental conditions play an important role in the measurement of these quantities. The geometrical parameters introduced by the experimental conditions are considered in the following section.

### 1.3.3 Effect of spatial coherence

The result obtained in the previous section assumes that the detector can sense intensity fluctuations strictly in a given direction. This means that the detector

collects light from single scattering wavevector. In practice, the detector has a finite spatial extent and collects light from a range of wavevectors  $\Delta \mathbf{k}$  given by [4],

$$\Delta \mathbf{k} = \mathbf{k}_s - \mathbf{k}_i = \mathbf{q} + \delta \mathbf{k}$$

Since the detector has a finite area many individual speckles would illuminate this area. This would result in an averaging out of the intensity fluctuations [5]. It is desirable to have an effective area of the order of the average speckle size. But this poses other problems like the count-rate falling to levels lower than the dark count of the detector. Thus, the effective area of the light detector has a significant bearing on the signal to noise ratio of the experiments. To analytically determine the effect of the detector area one requires detailed information of the experimental geometry. In DLS experiments, the scattering volume can be thought of as an extended incoherent source. If we consider the source to be a linear object, each point on this object emits light that arrives at the detector with a random phase. The net intensity recorded at detector depends upon the total phase. We consider the electric fields  $E(r)$  and  $E(r')$  at two points  $r$  and  $r'$  on the detection plane,

$$\begin{aligned} E(r) &= \sum_i E(i) \\ E(r') &= \sum_i E'(i) \end{aligned}$$

Where  $E(i)$  and  $E'(i)$  are the electric fields arising due to the  $i^{th}$  discrete source. A rough estimate of the coherence distance of this one-dimensional case is the distance beyond which the  $\langle E(r)E(r') \rangle$  correlation function decays appreciably. It has been shown that this distance is approximately given by [6],

$$l_c \approx \frac{\lambda}{\Theta}$$

Where  $\lambda$  is the wavelength of light and  $\Theta$  is the angle subtended by the source at a point on the detector plane.

If  $|r - r'| > l_c$ , the signals at these two points are uncorrelated. The *coherence area* can be defined as the area around the point  $r$  such that all points within it are partially

coherent with the point  $r$ . An estimate of this coherence area for three dimensional sources is [7, 8] is given by,

$$A_{coh} \approx \frac{\lambda^2}{\Omega}$$

Where  $\Omega$  is the solid angle subtended by the source at  $r$ .

When spatial coherence effects are taken in to account the intensity correlation function  $g_2(\tau)$  derived in the previous section gets modified in the following way

$$g_2(\tau) = 1 + \beta |g_1(\tau)|^2$$

Where  $\beta$  is a coherence factor and its value is less than one.. In principle, though it is possible to calculate  $\beta$  for a given geometry, its value is usually obtained directly from the correlogram. When  $\beta$  is close to unity the correlation function decays from a high initial value. This implies a high signal to noise ratio. When  $\beta \rightarrow 0$  there is very little decay of the autocorrelation function implying a low signal to noise ratio. In experiments, to get a high signal to noise ratio, a compromise has to be made between the effective detector area and the intensity of the scattered light falling on the detector. The effective area of the detector should be close to the coherence area but the intensity on the detector should be well above the noise level of the instrument.

In the next section we describe some of the methods we have used to analyze the scattered light intensity correlation functions.

### **1.3.4 Relaxation time from intensity autocorrelation functions**

The analysis of the intensity autocorrelation functions obtained in the experiment has to be done without having a *priori* knowledge of how many relaxation processes are present in the system and their respective strengths. The inversion of the autocorrelation function  $g_2(\tau)$  to obtain the relaxation time distribution function is mathematically an 'ill-posed' problem. When there is only one relaxation process in the system,  $|g_1(\tau)|^2$  decays as a single exponential. In the presence of multiple

relaxation processes,  $g_1(\tau)$  can be written as,

$$g_1(\tau) = \int_0^{\infty} G(\tau_r) e^{-\tau/\tau_r} d\tau_r$$

Where  $G(\tau_r)$  is the relaxation time distribution function that we seek to determine. The ill-posedness of this problem means that widely different models  $G(\tau_r)$  can be worked back to give nearly similar  $g_1(\tau)$ . We now discuss two commonly used techniques to analyze intensity autocorrelation functions.

### **Direct fitting of intensity autocorrelation functions to single or double exponential decays**

This is the simplest way of obtaining the relaxation time from the intensity autocorrelation function. This method should be used only when one is certain about the number of relaxation processes present in the system. For example, we consider the case when only one relaxation time is present in the system. As the name suggests this method involves fitting  $g_2(\tau)$  to a three parameter function of the form

$$a + be^{-(\tau/c)}$$

Where  $a$  is a baseline parameter,  $b$  is the amplitude of the decay that includes the coherence factor (a measure of the signal to noise ratio) and  $c$  is the relaxation time. This fitting would involve the use of non-linear fitting algorithms that require guess values of the parameters to be supplied at the beginning. Alternatively, since we are mainly interested in the relaxation time parameter  $c$  we can take a natural logarithm of  $(g_2(\tau) - a)$  and perform a straight line fit to the resulting equation.

$$\ln(g_2(\tau) - a) = \ln(b) - \left(\frac{1}{c}\right) \tau$$

The slope of this line is the inverse of the relaxation time. If the system has two relaxation times not very different from each other then one fits a sum of two exponential to  $g_2(\tau)$ . On the other hand, if the two relaxation times are well separated, it would be preferable to perform a piece wise linear fit to the two linear portions of  $\ln(g_2(\tau) - a)$  since polynomial fitting is more reliable than nonlinear fitting.

## Method of cumulants

This method is best suited to analyze particle sizing data where there is a narrow polydispersity in the size distribution. Here the natural logarithm of  $|g_1(\tau)|^2$  is expanded as a power series in delay time  $\tau$ .

$$\ln(|g_1(\tau)|^2) = A + B\tau + C\tau^2 \quad (1.10)$$

When plotted against  $\tau$ , the Y intercept equal to  $A$ , is a measure of the coherence factor  $\beta$  discussed previously and the slope equal to  $B$  is a measure of the average particle size. The coefficient  $C$  is a measure of the deviation from linearity and the polydispersity in the system. In fact,  $C/B^2$  is the polydispersity.

## 1.4 Dynamic light scattering from nematics

Nematic liquid crystals generally appear turbid. The turbid appearance of a nematic sample is due to the thermal fluctuations in the director. These director fluctuations are coupled to the dielectric tensor of the nematic. Each mode of the director fluctuation is characterized by a viscoelastic coefficient. By using the appropriate scattering geometry, it is possible to selectively detect intensity fluctuations due to a particular mode. An analysis of the intensity autocorrelation function yields the value of the viscoelastic coefficient associated with the particular mode. In the following section we derive the expression for the electric field scattered due the dielectric constant' fluctuations in the medium. This expression is later used to analyze light scattering from nematics.

### 1.4.1 Light scattering due to orientational fluctuations in the local dielectric tensor

We consider the scattering of light from a non-absorbing, non-conducting and non-magnetic medium [9]. The light incident on this medium is a plane wave whose electric field is given by,

$$\mathbf{E}_i(\mathbf{r}, t) = \mathbf{i}E_0 e^{\mathbf{k}_i \cdot \mathbf{r} - i\omega t}$$

where  $\mathbf{i}$  is the direction of polarization of the incident plane wave front and  $\omega$  is the angular frequency of light. We assume that the sample has spatio temporal fluctuations of the dielectric constant causing the incident plane wavefront to get scattered. The local dielectric tensor of the medium can be written as a sum of a constant part and a fluctuating part.

$$\underline{\epsilon} = \epsilon_0 \underline{\mathbf{I}} + \delta\underline{\epsilon}(\mathbf{r}, t)$$

Where  $\underline{\mathbf{I}}$  is a second rank unit tensor and  $\delta\underline{\epsilon}(\mathbf{r}, t)$  is the spatio-temporal dielectric tensor at  $\mathbf{r}$ . The field at the location of the detector  $\mathbf{R}$  is a sum of the incident and scattered fields. The total field is given by,

$$\mathbf{D} = \mathbf{D}_i + \mathbf{D}_s$$

$$\mathbf{E} = \mathbf{E}_i + \mathbf{E}_s$$

Where  $\mathbf{D}_i$  and  $\mathbf{E}_i$  are the incident displacement and electric fields,  $\mathbf{D}$ , and  $\mathbf{E}$ , are the scattered displacement and electric fields.

The second rank dielectric constant tensor  $\underline{\epsilon}$  relates the displacement and electric fields.

$$\mathbf{D} = \underline{\epsilon} \mathbf{E}$$

$$\mathbf{D}_i + \mathbf{D}_s = (\epsilon_0 \underline{\mathbf{I}} + \delta\underline{\epsilon})(\mathbf{E}_i)$$

$$\mathbf{D}_s = \epsilon_0 \underline{\mathbf{I}} \mathbf{E}_i + \delta\underline{\epsilon} \mathbf{E}_i$$

It is through this equation that fluctuations enter the analysis. The dielectric displacement at the detector depends not only on the scattered field but also on the product of the incident field and the local dielectric fluctuations. Using Maxwell's equations we can write a wave equation for the scattered displacement field vector as,

$$\nabla^2 \mathbf{D}_s - \left( \frac{\epsilon_0}{c^2} \right) \frac{\partial^2 \mathbf{D}_s}{\partial t^2} = -\nabla \times \nabla \times (\delta\underline{\epsilon} \mathbf{E}_i)$$

In terms of the Hertz vector the wave equation becomes

$$\nabla^2 \mathbf{\Pi} - \left( \frac{\epsilon_o}{c^2} \right) \frac{\partial^2 \mathbf{\Pi}}{\partial t^2} = -(\delta \underline{\epsilon} \mathbf{E}_i)$$

Where the Hertz vector is  $\mathbf{\Pi}$  is defined as

$$\nabla \times \nabla \times \mathbf{\Pi} = \mathbf{D}_s$$

We can solve the above equation using the Fourier transform method. The wave equation can be reduced to the Helmholtz equation using the properties of the Fourier transforms of derivatives [10]. The expression for the electric field at the detector polarized in the direction  $\mathbf{f}$  is given by

$$\mathbf{E}_s = \frac{E_o}{4\pi\epsilon_o R} e^{i(k_f R - \omega t)} \int_V \mathbf{f} \cdot (\mathbf{k}_f \times \mathbf{k}_f \times \delta \underline{\epsilon}(\mathbf{r}, t)) \cdot \mathbf{i} e^{i\mathbf{q} \cdot \mathbf{r}}$$

where  $V$  is the scattering volume and  $\mathbf{q} = \mathbf{k}_i - \mathbf{k}_s$ , is the scattering wave vector. The unit vectors  $\mathbf{i}$  and  $\mathbf{f}$  denote the initial and final directions of polarizations. Simplifying the double cross product in the above equation we get the final expression for the scattered field

$$\mathbf{E}_s = \left( -\frac{E_o k_f^2}{4\pi\epsilon_o R} \right) e^{i(k_f R - \omega t)} \delta \epsilon_{if}(q, t)$$

Where

$$\delta \epsilon_{if}(q, t) = \int_V \mathbf{f} \cdot \delta \epsilon(\mathbf{r}, t) \cdot \mathbf{i} e^{i\mathbf{q} \cdot \mathbf{r}} d^3r$$

is the  $if$  component of the fluctuating part of the dielectric tensor for the initial( $\mathbf{i}$ ) and final ( $\mathbf{f}$ ) polarization directions. Thus, one can obtain the magnitude of the scattered electric field arising due to the dielectric constant fluctuations in the medium. This relation is used while calculating the coupling between the director components and the dielectric constant tensor in a nematic liquid crystal.

## 1.4.2 Orientational fluctuations in a nematic liquid crystal

The equilibrium configuration for a nematic liquid crystal is one in which the director is uniformly aligned in a particular direction. Any deformation of this equilibrium

state costs excess free energy. This elastic *distortion free energy* is called the Frank free energy [11] given by,

$$F_d = \frac{1}{2} \int \{K_1(\nabla \cdot \mathbf{n})^2 + K_2(\mathbf{n} \cdot \nabla \times \mathbf{n})^2 + K_3(\mathbf{n} \times \nabla \times \mathbf{n})^2\} d^3r \quad (1.11)$$

Where  $\mathbf{n} \equiv \mathbf{n}(x,y,z)$  is the director field. The three terms in the integral represent the three basic distortions of the nematic, viz., the splay, twist and the bend.  $K_1$ ,  $K_2$  and  $K_3$  are the splay, twist and bend elastic constants respectively. Any arbitrary distortion of the nematic can be resolved in terms of these three independent distortions. We shall now consider small fluctuations of the director. This is shown in figure(1.8). We assume that in equilibrium the director,  $\mathbf{n}_o$ , is aligned along the z-axis.

$$\mathbf{n}(\mathbf{r}) = \mathbf{n}_o + \delta\mathbf{n}(\mathbf{r})$$

Where  $\delta\mathbf{n}(\mathbf{r})$  is the fluctuation. The components of  $\delta\mathbf{n}(\mathbf{r})$  are

$$\delta\mathbf{n}(\mathbf{r}) = (n_x(\mathbf{r}), n_y(\mathbf{r}), n_z = 0)$$

The different terms of equation(1.11) now become,

$$(\nabla \cdot \mathbf{n}) = \frac{\partial n_x}{\partial x} + \frac{\partial n_y}{\partial y}$$

$$(\mathbf{n} \cdot \nabla \times \mathbf{n}) = \frac{\partial n_x}{\partial y} - \frac{\partial n_y}{\partial x}$$

$$(\mathbf{n} \times \nabla \times \mathbf{n}) = \frac{\partial n_x}{\partial z} - \frac{\partial n_y}{\partial z}$$

The components of director fluctuation can be expressed as superpositions of individual modes.

$$n_x(\mathbf{r}) = \frac{1}{\Omega} \sum_{\mathbf{q}} n_x(\mathbf{q}) e^{-i\mathbf{q} \cdot \mathbf{r}} \quad (1.12)$$

$$n_y(\mathbf{r}) = \frac{1}{\Omega} \sum_{\mathbf{q}} n_y(\mathbf{q}) e^{-i\mathbf{q} \cdot \mathbf{r}} \quad (1.13)$$

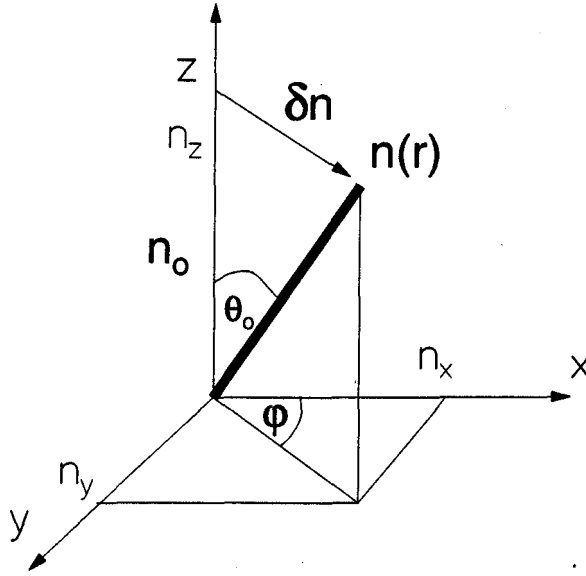


Figure 1.8: Schematic illustration of the director fluctuation at  $\mathbf{r}$

Where  $\Omega_0$  is a volume element and  $\mathbf{q}$  is the scattering wavevector.

Using equations (1.12) and (1.13) in the expression for free energy density we get,

$$\begin{aligned}
 F_D = \frac{1}{2\Omega_0} \sum_{\mathbf{q}} \{ & K_1 (|n_x(\mathbf{q})|q_x + |n_y(\mathbf{q})|q_y)^2 \\
 & + K_2 (|n_x(\mathbf{q})|q_y - |n_y(\mathbf{q})|q_x)^2 \\
 & + K_3 q_3^2 (|n_x(\mathbf{q})|^2 + |n_y(\mathbf{q})|^2) \} \quad (1.14)
 \end{aligned}$$

We now make a transformation into a co-ordinate system where  $F_d$  is diagonal and the energy in each mode can be written down.

The new co-ordinate system is obtained by rotating the old one about the z axis in such a way that  $\mathbf{q}$  lies in the x-z plane This is shown in figure(1.9). The basis vectors in the new co-ordinate system are  $(\mathbf{e}_1, \mathbf{e}_2)$ . The directions of the unit vectors  $\mathbf{e}_1$  and  $\mathbf{e}_2$  with respect to the direction of the scattering wave vector  $\mathbf{q}$  is given by

$$\mathbf{e}_1 \parallel \mathbf{q}$$

$$\mathbf{e}_2 \perp \mathbf{q}$$

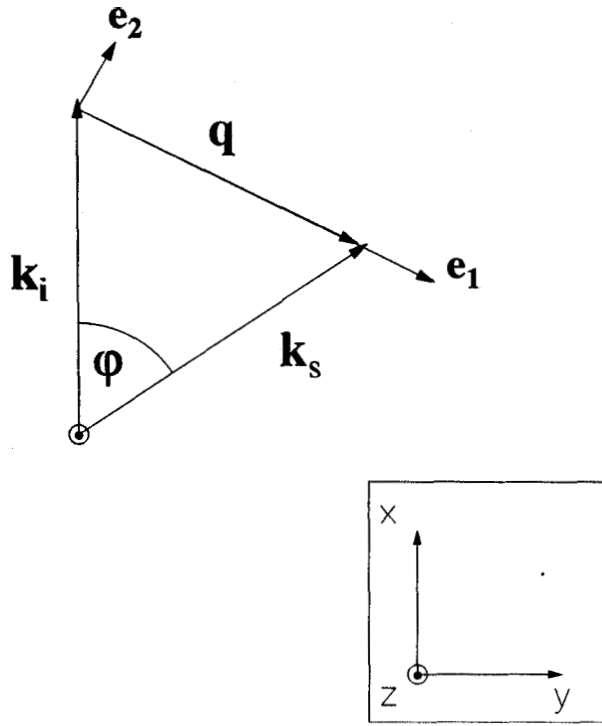


Figure 1.9: Illustrating the basis vectors in the  $\mathbf{e}_1, \mathbf{e}_2$  frame.  $\mathbf{q}$  is the scattering wavevector.

The fluctuation component in the new basis can be written as

$$\delta \mathbf{n}(\mathbf{q}) = \mathbf{e}_1 n_1(\mathbf{q}) + \mathbf{e}_2 n_2(\mathbf{q}) \quad (1.15)$$

The coefficients of  $K_1$  and  $K_2$  terms in equation(1.14) can be written respectively as,

$$\{|n_x(\mathbf{q})|q_x + |n_y(\mathbf{q})|q_y\}^2 = \{|\delta \mathbf{n}(\mathbf{q}) \cdot \mathbf{q}|\}^2$$

$$\{|n_x(\mathbf{q})|q_y - |n_y(\mathbf{q})|q_x\}^2 = \{|\delta \mathbf{n}(\mathbf{q}) \times \mathbf{q}|\}^2$$

In the expansions on the right hand sides

$$n_1(\mathbf{q})\mathbf{e}_1 \cdot \mathbf{q} + n_2(\mathbf{q})\mathbf{e}_2 \cdot \mathbf{q} \quad (1.16)$$

and

$$n_1(\mathbf{q})\mathbf{e}_1 \times \mathbf{q} + n_2(\mathbf{q})\mathbf{e}_2 \times \mathbf{q} \quad (1.17)$$

The second term in equation(1.16) is zero since  $\mathbf{e}_2 \perp \mathbf{q}$  and the first term in equation(1.17) is zero since  $\mathbf{e}_1 \parallel \mathbf{q}$ .

Thus the diagonalized form of the free energy density is,

$$F_d = \frac{1}{2\Omega_o} \sum_{\mathbf{q}} \{K_1 |n_1(\mathbf{q})|^2 q_{\perp}^2 + K_2 |n_2(\mathbf{q})|^2 q_{\perp}^2 + K_3 q_{\parallel}^2 (|n_1(\mathbf{q})|^2 + |n_2(\mathbf{q})|^2)\}$$

It can also be written as:

$$F_d = \frac{1}{2\Omega_o} \sum_{\mathbf{q}} \sum_{\alpha=1,2} |n_{\alpha}(\mathbf{q})|^2 (K_3 q_{\parallel}^2 + K_{\alpha} q_{\perp}^2) \quad (1.18)$$

Where  $\alpha=1,2$  are the two decoupled modes and  $K_{\alpha}$  is the elastic constant of the mode  $\alpha$ . According to the equipartition theorem each mode has the energy  $\frac{1}{2}k_B T$  and the thermal average of the square of its amplitude is given by,

$$\langle |n_{\alpha}(\mathbf{q})|^2 \rangle = \frac{k_B T}{K_3 q_{\parallel}^2 + K_{\alpha} q_{\perp}^2} \quad (1.19)$$

In nematic liquid crystals, fluctuations in the dielectric tensor are decided by director fluctuations. The restoring force for long wavelength fluctuations tend to zero as  $q \rightarrow 0$ . Thus, long wavelength fluctuations are easily excited in liquid crystals. The modes 1 and 2 represent the two decoupled modes of director fluctuations in nematics. The physical meaning of these modes in terms of the basic nematic deformations are discussed in the next section.

### 1.4.3 The decoupled modes of director fluctuation

In the  $(\mathbf{e}_1, \mathbf{e}_2)$  coordinate system the scattering wavevector  $\mathbf{q}$  is confined to the  $\mathbf{e}_1 - z$  plane. The sample is aligned with its director along the  $z$  direction. The tilt of the director due to any arbitrary fluctuations with scattering wavevector  $\mathbf{q}$  can be resolved in terms of displacements in two orthogonal planes, the  $\mathbf{e}_1 - z$  plane and the  $\mathbf{e}_2 - z$  plane. These orthogonal modes have been referred to as mode 1 and mode 2 in literature. These modes are illustrated in figure(1.10).

**Mode 1:** Here the director fluctuations are confined to the  $\mathbf{e}_1 - z$  plane. When  $\mathbf{q}$  is completely along  $\mathbf{e}_1$  the mode is a pure bend mode and when  $\mathbf{q}$  is along  $z$  the mode is a pure splay mode. In general the scattering wavevector will have both the  $\mathbf{e}_1$  and  $z$  components and the mode is the splay-bend mode.

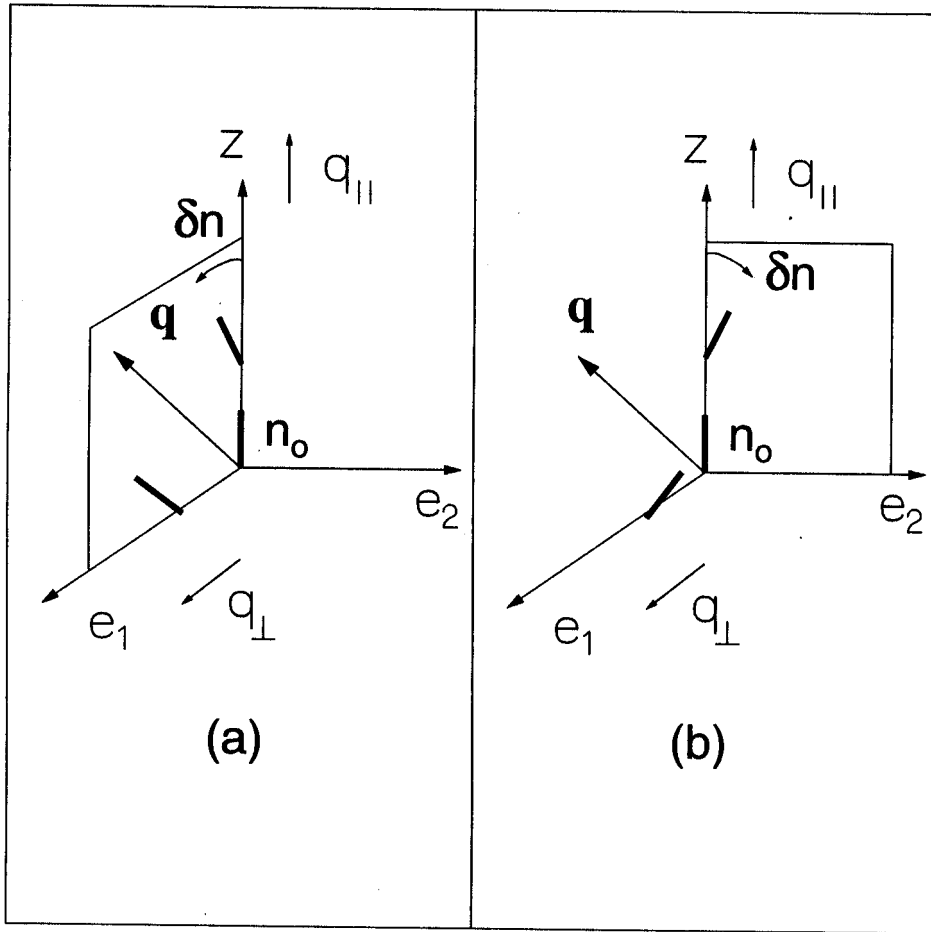


Figure 1.10: The decoupled nematic fluctuation modes. (a) Mode 1 is the splay-bend mode and (b) Mode 2 is the twist-bend mode.

**Mode 2:** If the director tilt is confined to the  $\mathbf{e}_2$ - $z$  plane, then a mode with wavevector along  $\mathbf{e}_1$  represents a pure twist mode and one with a wavevector along the  $z$  direction will represent a pure bend mode. Hence in general, this is twist-bend mode. Experimentally, it is possible to detect these modes individually by employing appropriate scattering geometries.

Having resolved arbitrary director fluctuations in terms of the decoupled modes 1 and 2 we now discuss the relation between the autocorrelation functions of the director components and the dielectric tensor of the nematic medium. The following section establishes the important relation between light scattering and the director fluctuations.

#### 1.4.4 The coupling between the director components and dielectric tensor

In a reference frame attached to the director, the dielectric tensor  $\underline{\epsilon}_m$  is given by,

$$\underline{\epsilon}_m = \begin{bmatrix} \epsilon_{\perp} & 0 & 0 \\ 0 & \epsilon_{\perp} & 0 \\ 0 & 0 & \epsilon_{\parallel} \end{bmatrix} \quad (1.20)$$

Here,  $\epsilon_{\parallel}$  is the extraordinary refractive index and  $\epsilon_{\perp}$  is the ordinary refractive index. The dielectric tensor for arbitrarily oriented director in the lab frame  $\underline{\epsilon}$  is given by the unitary transformation,

$$\epsilon = R^{-1} \underline{\epsilon}_m R$$

Where  $R$  is the Euler rotation matrix.

In tensor form, the nematic dielectric tensor in the lab frame  $(x, y, z)$  can be written as,

$$\epsilon_{xy} = \epsilon_{\perp} \delta_{xy} + \Delta\epsilon n_x n_y \quad (1.21)$$

$\Delta\epsilon$  is the dielectric anisotropy,  $\Delta\epsilon = \epsilon_{\parallel} - \epsilon_{\perp}$  and  $\delta_{x,y}$  is the Kronecker delta.

Let the directions of polarization of the incident and scattered light be  $\mathbf{i}$  and  $\mathbf{f}$  respectively, in the lab frame. The  $(\mathbf{i}, \mathbf{f})$  component of  $\mathbf{g}$  is given by,

$$\underline{\epsilon}_{if} = \begin{bmatrix} f_x & f_y & f_z \end{bmatrix} \underline{\epsilon} \begin{bmatrix} i_x & i_y & i_z \end{bmatrix} \quad (1.22)$$

When the director fluctuations are included, the dielectric tensor can be written as a sum of a spatially constant part (which does not contribute to light scattering) and a fluctuating part which can be written as,

$$\delta\epsilon_{if} = \Delta\epsilon [(\mathbf{i} \cdot \mathbf{n}_o)(\mathbf{f} \cdot \delta\mathbf{n}) + (\mathbf{i} \cdot \delta\mathbf{n})(\mathbf{f} \cdot \mathbf{n}_o)] \quad (1.23)$$

Where the term,  $(\mathbf{i} \cdot \delta\mathbf{n})(\mathbf{f} \cdot \delta\mathbf{n})$  which is of second order in fluctuations has been neglected.

Writing  $\delta\epsilon(\mathbf{q})$  in terms of the basis vectors  $\mathbf{e}_1$  and  $\mathbf{e}_2$  we can write,

$$\begin{aligned} \delta\epsilon(\mathbf{q}, t) &= (\Delta\epsilon) \left[ (\mathbf{i} \cdot \mathbf{n}_o)(\mathbf{f}) \cdot (\mathbf{e}_1 n_1(\mathbf{q}) + \mathbf{e}_2 n_2(\mathbf{q})) + (\mathbf{f} \cdot \mathbf{n}_o)(\mathbf{i}) \cdot (\mathbf{e}_1 n_1(\mathbf{q}) + \mathbf{e}_2 n_2(\mathbf{q})) \right] \\ &= (\Delta\epsilon) \left[ n_1(\mathbf{q}, t) G_1 + n_2(\mathbf{q}, t) G_2 \right] \end{aligned} \quad (1.24)$$

Where  $G_1$  and  $G_2$  are purely geometrical factors given by,

$$G_1 = (\mathbf{i} \cdot \mathbf{n}_o)(\mathbf{f} \cdot \mathbf{e}_1) + (\mathbf{f} \cdot \mathbf{n}_o)(\mathbf{i} \cdot \mathbf{e}_1) \quad (1.25)$$

$$G_2 = (\mathbf{i} \cdot \mathbf{n}_o)(\mathbf{f} \cdot \mathbf{e}_2) + (\mathbf{f} \cdot \mathbf{n}_o)(\mathbf{i} \cdot \mathbf{e}_2) \quad (1.26)$$

We can now relate the electric field autocorrelation function with the autocorrelation functions of the director fluctuations of the two independent modes.

$$\begin{aligned} \langle E(\mathbf{R}) E^*(\mathbf{R}, t + \tau) \rangle & \quad (1.27) \\ &= \left( \frac{k_s E_o}{4\pi R} \right)^2 \left[ G_1^2 \langle n_1(\mathbf{q}, t) n_1^*(\mathbf{q}, t + \tau) \rangle + G_2^2 \langle n_2(\mathbf{q}, t) n_2^*(\mathbf{q}, t + \tau) \rangle \right] e^{-i\omega\tau} \end{aligned}$$

The relaxation dynamics of the director fluctuations given by equation(1.15) is decided by the hydrodynamic theory of nematics. In the next section, we derive the final relation between the electric field autocorrelation function and the relaxation times of the different viscoelastic modes of the nematic.

### 1.4.5 Nematodynamics

We appeal to the hydrodynamic theory of relaxation of the director field as developed by Leslie and Ericksen to obtain the equation of motion for the director [12], [13] [14]. For this we need five viscosity coefficients to describe the viscous behavior of the nematic phase. The dynamics of the director is modeled on the damped simple harmonic oscillator. Hence the equation of motion of the component  $n_\alpha$ , of the director can be written as.

$$\eta_\alpha(\mathbf{q}) \frac{\partial}{\partial t} n_\alpha(\mathbf{q}, t) + K_\alpha n_\alpha(\mathbf{q}, t) = 0 \quad (1.28)$$

Where  $\eta_\alpha(\mathbf{q})$  is a component of viscosity and  $K_\alpha$  is the elastic term defined in equation(1.18).

We assume this equation to have a solution of the form

$$n_\alpha(\mathbf{q}, t) = n_\alpha(\mathbf{q}) e^{-(t/\tau_\alpha)}$$

Where  $\tau_\alpha$  is the relaxation time for the mode  $\alpha$ .

$$\frac{1}{\tau_\alpha} = \frac{K_3 q_{\parallel}^2 + K_\alpha q_{\perp}^2}{\eta_\alpha(\mathbf{q})} \quad (1.29)$$

The final expression for the electric field autocorrelation function becomes

$$\langle E(\mathbf{R}) E^*(\mathbf{R}, t + \tau) \rangle = \quad (1.30)$$

$$C \frac{K_B T}{V} \left[ G_1^2 \langle |n_1(\mathbf{q})|^2 \rangle e^{-(\tau/\tau_1)} + G_2^2 \langle |n_2(\mathbf{q})|^2 \rangle e^{-(\tau/\tau_2)} \right] e^{-i\omega\tau}$$

Where C is a time independent constant. In general the autocorrelation function will contain two relaxation times. By choosing the appropriate scattering geometry either  $G_1$  or  $G_2$  can be made to zero and the splay-bend or twist-bend modes can be observed individually. In experiments, modes have varying contributions to autocorrelation function at different wavevectors. In addition to choosing the right scattering geometry one should also chose the right scattering wavevector (equivalently the scattering angle) where the mode of interest has maximum contribution.

Equations(1.29) and (1.30) derived in this chapter will be used in the analysis of data in the experiments described in chapters **3,4** and 6 of this thesis.

# Bibliography

- [1] S. K. Muthu. Probability and Errors for the Physical Sciences. Orient Longman Limited, New Delhi, (1982).
- [2] P. A. Lemieux and D. J. Durian. *J. Opt. Soc. Am.*, 16, 1651, (1999).
- [3] A. V. Balakrishnan. Introduction to Random Processes in Engineering. Wiley, (1995).
- [4] W. I. Goldberg. Dynamic light scattering. *Am. J. Phys.*, 67, 1152, (1999).
- [5] H. Z. Cummins and H. L. Swinney. Progress in Optics, page 135. North-Holland, London, (1970).
- [6] H. Lipson S. G. Lipson and D. S. Tannhauser. Optical Physics. Cambridge University Press, Cambridge, (1995).
- [7] J. B. Lastovka V. Degiorgio. *Phys. Rev. A*, A4, 2033, (1971).
- [8] A. T. Forrester. *J. Opt. Soc. Am.*, 51, 253, (1961).
- [9] B. J. Berne and R. Pecora. Dynamic Light Scattering. Wiley, New York, (1976).
- [10] V. D. Barger and M. G. Olsson. Classical Electricity and Magnetism: A Contemporary Perspective. Allyn and Bacon, Boston, (1987).
- [11] P. G. de Gennes and J. Prost. The Physics of Liquid Crystals, 2nd. edition Clarendon press, Oxford, (1993).
- [12] F. M. Leslie. Advances in *Liquid Crystals*, volume 4, chapter Theory of Flow Phenomenon in Liquid Crystals. The Chemical Society, London, (1983).

- [13] Ericksen. *Advances in Liquid Crystals*, volume 4, chapter Equilibrium Theory of Liquid Crystals. The Chemical Society, London, (1983).
- [14] S. Chandrasekhar. *Liquid Crystals*. 2nd. edition, Cambridge University press, Cambridge, (1992).

